Experimental Study on Axial Compression Behavior of RC Columns Under Rapid Loadings

X. Zeng & B. Xu
College of Civil Engineering, Hunan University, Yuelu Mountain, Changsha, Hunan 410082, P.R.China

X.Z. Zhang
KPFF Consulting Engineers, Los Angeles, CA, USA

SUMMARY:
In this study, experimental study on six RC columns with different slenderness ratios under axial rapid loading was conducted to investigate the axial compression behaviour of RC columns considering the effect of strain rates. The failure pattern of the specimens and the relations of axial loading versus the axial deformation were described. From the test results, the specimens under static and dynamic axial loadings have similar failure model and the strength and the corresponding axial deformation of the RC columns increase with the strain rate. Finally, based on the formula proposed by the CEB-FIP model code considering dynamic strength increase factor for concrete materials, the theoretical dynamic strength increasing factor for the specimens was determined and compared with the experimental measurements. The difference between the forecasted dynamic load-carrying capacity and the measurement for specimens with larger slenderness ratio is relatively larger that of specimens with smaller slenderness ratio.

Keywords: RC columns, axial compression, rapid loading, strain rate effect, slenderness ratio

1. GENERAL INSTRUCTIONS

As early as in 1917, Abram (1917) discovered that the strain rate increases the compression strength of concrete materials. The strain rate plays an important role in the behaviour of RC members under dynamic loading and experimental and analytical study on the dynamic behaviour of concrete materials and structures under rapid loadings has received much attention (Bischoff and Perry, 1991; Malvar and Ross, 1998). It is important to predict correctly the behaviour of concrete structures under strong dynamic loadings such as earthquake where the high strain rates affect the mechanical behaviour of the structure. Bertero (1972) predicted that for a very rigid structure with a fundamental natural period of about 0.1 s, the strain rate at some critical regions can be as high as 0.025/s. Therefore, it is very significant to investigate the effect of loading rate on the behaviour of RC members.

In order to investigate the behaviour of RC columns in vertical earthquake actions, the axial compression behaviour of RC columns under rapid loading was studied (Reinschmidt et al., 1964; Iwai et al, 1988). The study results show the increase in compression strength of RC column due to strain rate effect. In the past years, experimental study was carried out to investigate the behaviour of RC columns under constant axial force and rapid lateral loading (Orozco and Ashford, 2002; Tagami et al., 2005).

In this study, further experimental study on the axial compression behaviour of RC columns with different slenderness ratio and loading rates was carried out. The final failure patterns, the load-carrying capacity and the corresponding axial deformation were compared with that under static loading. Finally, based on the formula proposed by the CEB-FIP model code considering dynamic strength increase factor for concrete materials, the theoretical dynamic strength increasing factor for the specimens was determined and compared with the experimental measurements.

2. TEST PROGRAM

A total of six specimens with two different slenderness ratios were tested. The test matrix is given in Table 2.1 and the design of the specimens in detail is shown in Fig. 2.1. The dimension of the cross section of the columns is determined according to the capacity of the dynamic testing machine employed in this study. All specimens have an identical cross section of 250mm×250mm. Ribbed steel bar with a diameter of 16mm was used as longitudinal steel rebar and round steel bar with a diameter of 8mm as stirrup rebar with a spacing of 150 mm. Two bolts at each end were pre-embedded into the concrete to connect the specimen with the test machine. In order to avoid the failure of concrete at the two ends of the specimens under dynamic loadings due to local stress concentration, the two ends of the columns were reinforced with four steel reinforcing mesh within the length of 225 mm. Moreover, steel jackets were also employed to strengthen the concrete within the 490 mm region from the two ends. Among each group of specimens with identical slenderness ratio, two specimens were tested under rapid axial loading and the rest one was loaded statically. The loading rate for each specimen is shown in Table 2.1.

Table 2.1. Test Matrix

Group	Specimens	Cross section (mm×mm)	*L*/*D*	Average loading rate (mm/s)
One	S12	250×250	12	Pesudo-static
	D12-1			45
	D12-2			23
Two	S22		22	Pesudo-static
	D22-1			83
	D22-2			63

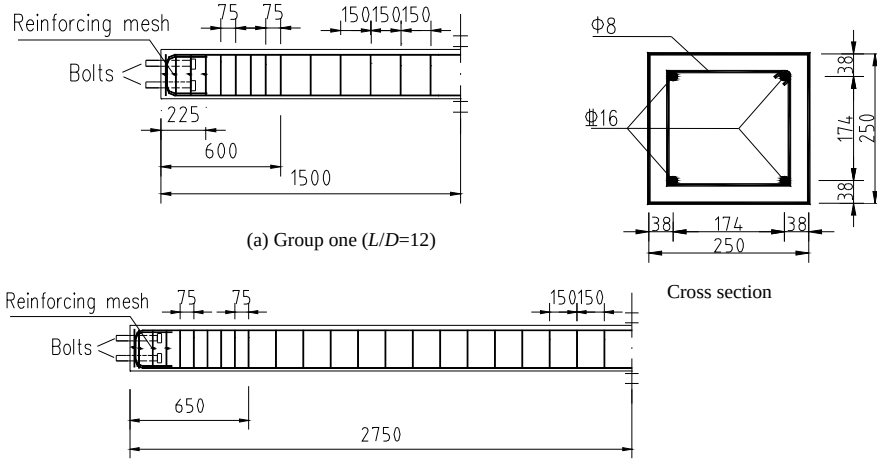

(a) Group one (*L*/*D*=12)

Cross section

(b) Group two (*L*/*D*=22)

Elevation

Figure 2.1. Design of the specimen in detail

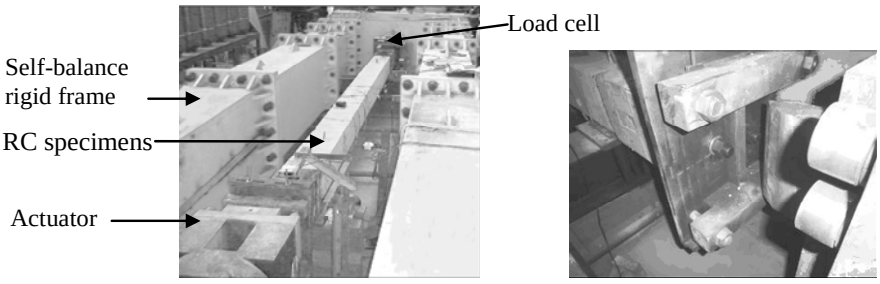

Elevation

Knife edge pin

Figure 2.2. Test setup

Test setup is shown in Fig. 2.2. All specimens were installed in a self-balanced rigid frame and were supported by knife edge pins at the two ends and tested using an electro-hydraulic servo-controlled testing system with a maximum static load capacity of 450 tones and a maximum dynamic capacity of 350 tones at a loading speed of 1.0m/s for actuator stroke. Displacement control mode was adopted in this test by setting the maximum displacement and loading frequency. The specimens were loaded in axial direction by the electro-hydraulic actuator and a load cell was placed at the fixed pin end to measure the axial load. Strain gauges were placed along the longitudinal steel reinforcement to measure the strain of the rebar under loadings. The load, axial deformation and strain were measured synchronously with a sampling rate of 1kHz.

All specimens were casted simultaneously. In the concrete mix, the fine aggregate was silica-based sand and the coarse aggregate was gravel with the maximum size of 30mm from local area. The yield strength and ultimate strength of the longitudinal steel bar are 483.0MPa and 617.9MPa respectively and the yield strength and ultimate strength of the stirrup bar were 344.6Mpa and 421.6MPa respectively. The compression strength of concrete was 55.0 MPa.

3. TEST RESULT AND DISCUSSIONS

3.1 Failure Pattern

The failure patterns of the specimens with different slenderness ratio and loading rates are shown in Fig. 3.1. It seems that no difference exists in failure patterns when the specimens with same slenderness ratio are under static load and rapid loading. Concrete in the middle of the specimens crushed severely and the longitudinal steel bars between stirrups buckled at the position of concrete crush. Close to the buckling longitudinal steel bars, either stirrups ruptured or the end hook of the stirrups with 135 degree was pulled out of the longitudinal bars under the large inelastic deformation.

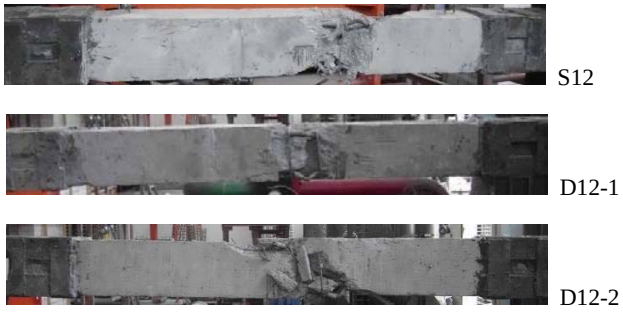

(a) Group one (L/D=12)

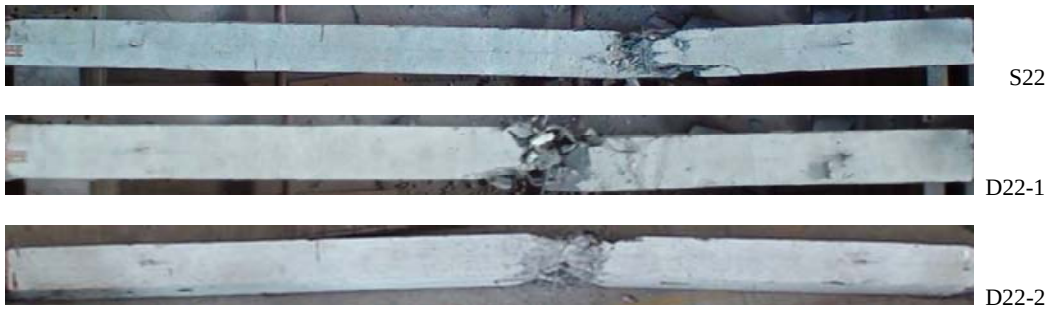

(b) Group two (L/D=22)

Figure 3.1. Failure patterns of specimens with different slenderness ratio and loading rates

3.2 Relations of Axial Force versus Axial Displacement

The relation between the axial force versus axial displacement of the tested specimens are shown in Fig. 3.2. The load-carrying capacity and the corresponding axial deformation of each specimen are shown in Table 3.1. It is clear that the dynamic axial strength and the corresponding axial deformation increased when compared with the static values. The load-carrying capacity of the axially loaded specimens has an average increase of 13.5%, 22.5% for group one and two, respectively. The axial deformation corresponding to the ultimate axial force under rapid loading for the specimens is 14% to 19% and 31% to 37% higher than that under static load for group one and group two respectively. In each group, there is no significant difference in strength and axial deformation at ultimate axial force between the two specimens under rapid loading. The ascending branch of the axial force versus axial deformation curve for each group seems consistent. All specimens failure in a brittle pattern and the descending branch of the axial force versus axial deformation curve fall down sharply.

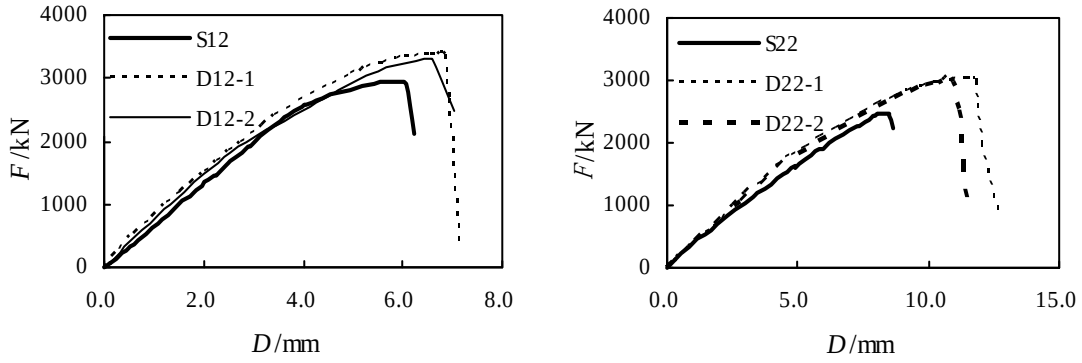

Figure 3.2. Relationship of axial load versus axial displacement

Table 3.1. Test Results on Load-carrying Capacity and the Corresponding Axial Deformation

Group	Specimens	Average loading rate (mm/s)	P_{emax}(kN)	DIF_{eP}	D_{eu}(mm)	DIF_{eD}
One	S12	Pesudo-static	2941	1.00	5.7	1.00
	D12-1	45	3390	1.15	6.8	1.19
	D12-2	23	3304	1.12	6.5	1.14
Two	S22	Pesudo-static	2469	1.00	8.3	1.00
	D22-1	83	3030	1.23	11.4	1.37
	D22-2	63	3020	1.22	10.9	1.31

Note: P_{emax} denotes the experimental axial load-carrying capacity.
DIF_{eP} denotes dynamic increasing factor of load-carrying capacity.
D_{eu} denotes the experimental axial deformation at peak axial force.
DIF_{eD} denotes dynamic increasing factor of the axial deformation at peak axial force.

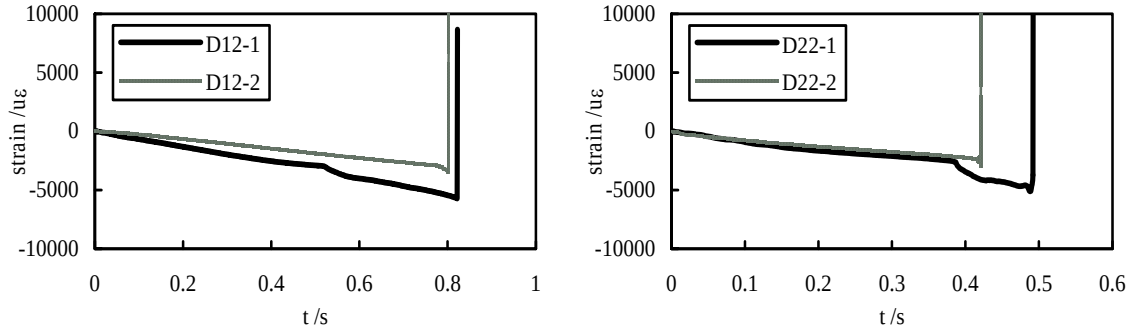

Figure 3.3. Time history of strain of longitudinal steel

From Table 3.1, it can be seen that both of the dynamic and pseudo-static load-carrying capacities of the specimens with smaller slenderness ratio are greater than them of the specimens with larger slenderness ratio. Considering the dynamic increasing factor of the two groups, it can be found that the

dynamic increasing factor of load-carrying capacity of slender specimens is larger than that of the shorter specimens. Based on the measurement of longitudinal steel strain measurements in the middle of the specimens in the test shown in the Fig. 3.3, the average strain rates reached to $0.0070s^{-1}$ and $0.0040s^{-1}$ for D12-1 and D12-2 respectively, and $0.0068s^{-1}$ and $0.0055s^{-1}$ for D22-1 and D22-2 respectively. The strain rate of the specimens of both group one and two is in the same order and the corresponding difference in the material strength due to the strain rate in this test is not obvious. So the difference in the dynamic increase in load-carrying capacity between group one and group two may be due to the different effect of inertia effect for the specimens with different slenderness ratios. From Figure 3.2, it also can be seen that the dynamic increasing factor of axial deformation corresponding to the load-carrying capacity of the slender specimens is larger than that of the shorter specimens.

4. AXIAL LOAD-CARRYING CAPACITY FORECAST UNDER RAPID LOADING

According to the AASHTO LRFD Bridge Design Specification, the static nominal axial resistance P_{sn} of each specimen can be determined in Eqn. 4.1.

$$P_{sn}=\chi(0.85f_{sc}(A_g- A_{st})+f_{sy}A_{st}) \tag{4.1}$$

Considering the strength increase of concrete under dynamic loading, the dynamic nominal axial resistance P_{dn} of each specimen can be described in Eqn. 4.2.

$$P_{dn}=\chi(0.85f_{dc}(A_g- A_{st})+f_{dy}A_{st}) \tag{4.2}$$

where:
χ = the factor considering the usable resistance of compression members to allow for unintended eccentricity
f_{sc}, f_{dc} = the static and dynamic compression strength of concrete (MPa)
f_{sy}, f_{dy} = the static and dynamic yield strength of longitudinal reinforcement (MPa)
A_g = gross area of section (mm^2)
A_{st} = total area of longitudinal reinforcement (mm^2)

According to the provisions in CEB-FIP MODEL CODE (1990), the dynamic increasing factor (DIF) of concrete strength are 1.13 and 1.11 corresponding to 0.0070 s^{-1} and 0.0040 s^{-1}. Li (2010) studied the dynamic properties of reinforcing rebar of various grade in China within the range of strain rate from 2.5×10^{-4} s^{-1} to 2.5×10^{-1} s^{-1} and proposed a DIF model for rebar. Based on the study by Li (2010), the DIFs of the employed rebar in this study are 1.017 and 1.014 corresponding to the strain rate of 0.0070 s^{-1} and 0.0040 s^{-1}, accordingly. Using Eqn.(4.1) and (4.2), theoretical dynamic increasing factor of strength of the columns $DIF_{cP}=P_{dn}/P_{sn}$ for group one and group two are between 1.11 and 1.10.

Comparing the theoretical value DIF_{cP} and experimental value DIF_{eP}, the differences between them are about 0.01-0.02 and 0.11-0.12 for group one and group two, respectively. The predicted value DIF_{cP} is very close to the experimental value DIF_{eP} for group one. For the specimens in group two with a large slenderness ratio, the difference between DIF_{cP} and DIF_{eP} becomes larger. The effects of the strain rate and the inertia for slender specimens should be studied in detail in the future.

5. CONCLUSIONS

In this study, tests on the axial compression behavior of RC columns with different slenderness ratios and under different loading rates were carried out. The final failure patterns, load-carrying capacity and the corresponding axial deformation were compared with them under pseudo-static loading. Moreover, the load-carrying capacities of the specimens considering the strain rate effects were forecast based on the AASHTO LRFD Bridge Design Specification and the dynamic increasing factor of concrete material strength proposed by the CEB-FIP model code.

Based on the test results, the following conclusions can be made.

(1) The failure pattern of RC specimens under axial pseudo-static and dynamic loadings is similar for specimens of both groups.

(2) The high strain rate increases both the load-carrying capacity and the corresponding axial deformation of the specimens of both groups. Both of the dynamic and pseudo-static load-carrying capacities of the specimens with smaller slenderness ratio are greater than that of the specimens with larger slenderness ratio.

(3) Both the dynamic increasing factor of load-carrying capacity and the corresponding axial deformation of slender specimens in this study are larger than them of the shorter specimens, even though the strain rate of the specimens of group one and group two is in the same order of magnitude.

(4) By using CEB-FIP model code (1990) considering the dynamic strength increase factor for concrete under high strain rate loading, the predicted value for group one is close to experimental value, but for group two with larger slenderness ratio the difference between the predicted value and experimental value is obvious. The slenderness also plays important roles in dynamic load-carrying capacity of RC columns. Further study should be carried out in order to study the effects of slenderness ratio on the dynamic behavior of RC structures.

AKCNOWLEDGEMENT

The authors gratefully acknowledge the support provided NSFC Key Project of the Major Research Program of Dynamic Disaster of Major Engineering Structure (No.90715033 and No. 91015007). Partial support by the Program for New Century Excellent Talents in University (No.NCET-08-0178), Ministry of Education, China, and the Fundamental Research Funds for the Central Universities at Hunan University to the second author is also appreciated.

REFERENCES

Abrams, D.A. (1917). Effect of rate of application of load on the compressive strength of concrete. *Proceedings ASTM*. **17: Part 2**, 146-165.

Bischoff, P.H. and Perry, S.H. (1991). Compressive behaviour of concrete at high strain rates. *Materials and Structures*. **24: 6**, 425-450.

Malvar, L. and Ross, C. (1998). Review of strain rate effects for concrete in tension. *ACI Material Journal*. **95: 6**, 735-739.

Bertero, V.V. (1972). Experimental studies concerning reinforced, prestressed and partially prestressed concrete structures and their elements. *Introductory Report, Symposium on Resistance and Ultimate Deformability of Structures Acted on by Well Defined Repeated Loads*. 67-99.

Tagami, J., Suzuki, N., Kaneko, T. and Maruta, M. (2005). Dynamic loading test of reinforced concrete columns for identification of strain rate effect. *Research Report, Proceedings of the First NEES/E-Defense Workshop on Collapse Simulation of Reinforced Concrete Building Structures*. **Session 7**, 291-304.

Orozco, G.L. and Ashford, S.A. (2002). Effects of large velocity pulses on reinforced concrete bridge columns. *PEER Report.*

Reinschmidt, K.F., Hansen, R.J. and Yang, C.Y. (1964). Dynamic tests of reinforced concrete columns. *ACI Journal Proceedings.* **61: 3**, 317-334.

Iwai, S., Minami, K. and Wakabayashi, M. (1988). Stability of slender reinforced concrete members subjected to static and dynamic loads. *Proceedings of the Ninth World Conference on Earthquake Engineering.* **Vol III:** 901-906.

Li, M. and Li, H. (2010). Dynamic test and constitutive model for reinforcing steel. *China Civil Engineering Journal*. **43: 4**, 70-75.